ISSN 1070-3284, Russian Journal of Coordination Chemistry, 2014, Vol. 40, No. 10, pp. 740–747. © Pleiades Publishing, Ltd., 2014.
Original Russian Text © Yu.A. Bryleva, L.A. Glinskaya, I.V. Korol'kov, A.S. Bogomyakov, M.I. Rakhmanova, D.Yu. Naumov, T.E. Kokina, S.V. Larionov, 2014, published in Koordinatsionnaya Khimiya, 2014, Vol. 40, No. 10, pp. 623–630.

Syntheses, Structures, Magnetic Properties, and Photoluminescence of Compounds $Ln(2,2'\text{-}Bipy)(C_4H_8NCS_2)_3 \cdot 0.5CH_2Cl_2$ (Ln = Sm, Eu, Tb, Dy, and Tm)

Yu. A. Bryleva[a], *, L. A. Glinskaya[a], I. V. Korol'kov[a, b], A. S. Bogomyakov[c], M. I. Rakhmanova[a], D. Yu. Naumov[a], T. E. Kokina[a, b], and S. V. Larionov[a, b]

[a] *Nikolaev Institute of Inorganic Chemistry, Siberian Branch, Russian Academy of Sciences, pr. akademika Lavrent'eva 3, Novosibirsk, 630090 Russia*

[b] *Novosibirsk State University, Pirogova st. 2, Novosibirsk, 630090 Russia*

[c] *International Tomography Center, Siberian Branch, Russian Academy of Sciences, Novosibirsk, 630090 Russia*

**e-mail: tapzu_bryleva@mail.ru*

Received February 26, 2014

Abstract—Five compounds of the composition $Ln(2,2'\text{-}Bipy)(C_4H_8NCS_2)_3 \cdot 0.5CH_2Cl_2$ (Ln = Sm (**I**), Eu (**II**), Tb (**III**), Dy (**IV**), and Tm (**V**); 2,2'-Bipy = 2,2'-bipyridine) are synthesized. According to the X-ray diffraction data (CIF file CCDC 986259), the crystal structure of compound **I** consists of molecules of the mononuclear complex $[Sm(2,2'\text{-}Bipy)(C_4H_8NCS_2)_3]$ and solvate molecules CH_2Cl_2 (2 : 1). The coordination polyhedron N_2S_6 of the Sm atom is a distorted tetragonal antiprism. The X-ray diffraction analysis shows that compounds **I–V** are isostructural. The magnetic properties of compounds **I–V** are analyzed in the temperature range from 2 to 300 K. At 300 K compounds **I** and **III** are photoluminescent in the visible spectral range. The photoluminescence intensity of compound **I** considerably exceeds that of complex **III**.

DOI: 10.1134/S1070328414100029

INTRODUCTION

Lanthanide (Ln) complexes with organic ligands are widely used for the production of luminescence devices [1–5]. The most part of works is devoted to the study of the luminescence of Ln complexes with O- and N-donor ligands. The studies of the luminescence of the Ln complexes with S-containing ligands have started only recently. The luminescent Ln compounds containing the monothiolate ligands were described [6–9]. Dithiolate ligands, in particular, dithiocarbamate ions bearing the NCS_2^- group, are among promising sulfur-containing ligands for the synthesis of luminescent Ln complexes. Complex $Na[Eu(S_2CNMe_2)_4] \cdot 3.5H_2O$ was shown to possess photoluminescence (PL) only at low temperatures (<100 K) [10]. It is known that the introduction of fluorophores, nitrous heterocycles, in particular, 1,10-phenanthroline (Phen) and 2,2'-bipyridine (2,2'-Bipy), into the composition of Ln complexes increases the PL intensity of the compounds. The syntheses and structures of heteroligand complexes $[Eu(L)(Et_2NCS_2)_3]$ (L = Phen, 2,2'-Bipy) were described [11, 12]. These complexes and $[Eu(Phen)(Ph_2NCS_2)_3]$ were found to exhibit PL at 300 K [13]. The PL of the Ln (La, Pr, Sm, Eu, Gd, Tb, Dy) complexes containing ligands $R_2NCS_2^-$ (R = Et, *iso*-Bu, Bz) and 2,2'-Bipy, Phen, and 5-Cl-Phen was studied at 300 K [14]. The heteroligand Ln complexes with pyrrolidinedithiocarbamate ions ($C_4H_8NCS_2^-$),) bearing the fragment of nitrogen heterocycle and Phen were synthesized [15–18]. We found that the complexes with Ln = Sm, Eu, Tb, Dy, and Tm exhibited PL [19]. In addition, the magnetic properties of these complexes were studied. Complex $Eu(2,2'\text{-}Bipy)(C_4H_8NCS_2)_3$, whose magnetic properties and PL remain unstudied, has been synthesized previously [18]. We synthesized solvate (2 : 1) $Sm(2,2'\text{-}Bipy)(C_4H_8NCS_2)_3 \cdot 0.5CH_2Cl_2$ (**I**) with significant PL [20].

The purpose of this work is the synthesis and investigation of the structures, magnetic properties, and PL of a series of heteroligand lanthanide complexes (Ln = Sm (**I**), Eu (**II**), Tb (**III**), Dy (**IV**), and Tm (**V**)) with $C_4H_8NCS_2^-$ ions and 2,2'-Bipy as a fluorophore.

EXPERIMENTAL

The following reagents were used for the syntheses of complexes **I–V**: $Sm(NO_3)_3 \cdot 6H_2O$ (analytical grade); $Eu(NO_3)_3 \cdot 6H_2O$ and $Tm(NO_3)_3 \cdot 4H_2O$ (reagent grade); $Tb(NO_3)_3 \cdot 5H_2O$ and $Dy(NO_3)_3 \cdot 5H_2O$ (high-purity grade); 2,2'-Bipy (analytical grade); and $C_4H_8NCS_2NH_4$ (Aldrich). The solvents used were *iso*-PrOH (special purity grade) and CH_2Cl_2 (reagent grade).

Synthesis of complex I. A solution of $C_4H_8NCS_2NH_4$ (0.32 g, 2.0 mmol) in 25 mL of an *iso*-PrOH–CH_2Cl_2 (2 : 3 vol/vol) mixture was added to a solution of $Sm(NO_3)_3 \cdot 6H_2O$ (0.22 g, 0.5 mmol) in *iso*-PrOH (3 mL) with stirring. The formed precipitate of NH_4NO_3 was filtered off, and a solution of 2,2'-Bipy (0.08 g, 0.5 mmol) in *iso*-PrOH (3 mL) was added to the filtrate. The mixture was stirred for 2 h. A light yellow precipitate was filtered off with suction, washed with *iso*-PrOH, and dried in a drying box over anhydrone. The product was recrystallized from CH_2Cl_2 (20 mL). The yield was 0.24 g (60%).

For $C_{25.5}H_{33}N_5S_6ClSm$
anal. calcd., %: C, 38.9; H, 4.2; N, 8.9; Cl, 4.5.
Found, %: C, 38.7; H, 4.2; N, 8.6; Cl, 4.3.

Complexes II–V were synthesized according to the procedure described above. The yields were 30, 30, 40, and 40%, respectively.

For $C_{25.5}H_{33}N_5S_6ClEu$ (**II**)
anal. calcd., %: C, 38.8; H, 4.2; N, 8.9; Cl, 4.5.
Found, %: C, 38.6; H, 4.2; N, 8.6; Cl, 4.4.

For $C_{25.5}H_{33}N_5S_6ClTb$ (**III**)
anal. calcd., %: C, 38.5; H, 4.2; N, 8.8; Cl, 4.5.
Found, %: C, 38.8; H, 4.2; N, 8.9; C, 4.5.

For $C_{25.5}H_{33}N_5S_6ClDy$ (**IV**)
anal. calcd., %: C, 38.3; H, 4.2; N, 8.8; Cl, 4.4.
Found, %: C, 37.5; H, 4.1; N, 8.5; Cl, 4.3.

For $C_{25.5}H_{33}N_5S_6ClTm$ (**V**)
anal. calcd., %: C, 38.0; H, 4.1; N, 8.7; Cl, 4.4.
Found, %: C, 37.5; H, 3.9; N, 8.4; Cl, 4.4.

Analyses to C, H, N were carried out on an Euro EA 3000 analyzer, and Cl was determined according to Scheniger with the titrimetric end. IR spectra at 400–3800 cm^{-1} were recorded in KBr pellets on a Scimitar FTS2000 spectrophotometer.

X-Ray diffraction analysis of complex I. Single crystals suitable for X-ray diffraction analysis were grown by the slow evaporation of a solution of compound **I** in CH_2Cl_2. The unit cell parameters and reflection intensities were measured at a low temperature (150 K) on a Bruker X8 Apex CCD automated diffractometer equipped with a two-coordinate detector using the standard procedure (MoK_α radiation, $\lambda = 0.71073$ Å, graphite monochromator). The composition of the single crystal obtained from the X-ray diffraction data coincided with the composition of polycrystals of compound **I** established on the basis of the elemental analysis data. The crystallographic characteristics, X-ray diffraction experimental details, and the structure refinement data for compound **I** are given in Table 1. The structure was solved by a direct method and refined by full-matrix least squares for F^2 in the anisotropic approximation (for non-hydrogen atoms) using the SHELXL-97 program package [21]. The positions of all hydrogen atoms were determined from difference Fourier syntheses and included into the refinement in the riding model. The structure refinement revealed disordering of the atoms of the CH_2Cl_2 molecules over two positions, whose site occupancy was 0.5. Selected interatomic distances and bond angles are listed in Table 2.

Table 1. Crystallographic characteristics and the experimental and structure refinement details for compound **I**

Parameter	Value
FW	786.72
Crystal system	Monoclinic
Space group	$P2_1/n$
a, Å	10.1401(3)
b, Å	19.5406(7)
c, Å	16.0701(4)
β, deg	101.950(1)
V, Å^3	3115.2(2)
Z; ρ_{calcd}, g/cm^3	4; 1.680
μ, mm^{-1}	2.399
Crystal sizes, mm	0.25 × 0.22 × 0.008
Scan θ range, deg	1.66–26.37
Number of measured reflections	19781
Number of independent reflections	6339
R_{int}	0.0237
Number of reflections with $I > 2\sigma(I)$	5750
Number of refined parameters	361
Goodness-of-fit for F^2	1.061
R factor ($I > 2\sigma(I)$)	$R_1 = 0.0222$ $wR_2 = 0.0545$
R factor (for all I_{hkl})	$R_1 = 0.0259$ $wR_2 = 0.0556$
Residual electron density (max/min), e/Å^3	1.294/–1.038

The full tables of atomic coordinates, bond lengths, and bond angles were deposited with the Cambridge Crystallographic Data Centre (CCDC 986259;

Table 2. Selected interatomic distances (d, Å) and bond angles (ω, deg) in the structure of compound **I***

Bond	d, Å	Angle	ω, deg
Sm(1)–N(1P)	2.591(2)	N(1P)Sm(1)N(2P)	62.63(6)
Sm(1)–N(2P)	2.608(2)	N(1P)Sm(1)S(11)	78.50(5)
Sm(1)–S(11)	2.8505(6)	N(2P)Sm(1)S(11)	78.09(5)
Sm(1)–S(22)	2.8601(6)	N(1P)Sm(1)S(22)	153.74(5)
Sm(1)–S(31)	2.8638(7)	N(2P)Sm(1)S(22)	142.80(5)
Sm(1)–S(12)	2.8641(6)	S(11)Sm(1)S(22)	108.94(2)
Sm(1)–S(32)	2.8924(6)	N(1P)Sm(1)S(31)	93.87(5)
Sm(1)–S(21)	2.9042(7)	N(2P)Sm(1)S(31)	75.18(5)
S(11)–C(11)	1.722(2)	S(11)Sm(1)S(31)	152.72(2)
S(12)–C(11)	1.720(3)	S(22)Sm(1)S(31)	89.53(2)
S(21)–C(21)	1.727(2)	N(1P)Sm(1)S(12)	81.62(5)
S(22)–C(21)	1.711(2)	N(2P)Sm(1)S(12)	131.77(5)
S(31)–C(31)	1.724(2)	S(11)Sm(1)S(12)	63.13(2)
S(32)–C(31)	1.723(2)	S(22)Sm(1)S(12)	79.87(2)
N(1P)–C(1P)	1.344(3)	S(31)Sm(1)S(12)	142.28(2)
N(1P)–C(5P)	1.345(3)	N(1P)Sm(1)S(32)	75.93(5)
N(2P)–C(10P)	1.332(3)	N(2P)Sm(1)S(32)	117.30(5)
N(2P)–C(6P)	1.348(3)	S(11)Sm(1)S(32)	137.77(2)
N(11)–C(11)	1.330(3)	S(22)Sm(1)S(32)	82.69(2)
N(11)–C(15)	1.475(3)	S(31)Sm(1)S(32)	62.47(2)
N(11)–C(12)	1.478(3)	S(12)Sm(1)S(32)	80.23(2)
N(21)–C(21)	1.324(3)	N(1P)Sm(1)S(21)	144.11(5)
N(21)–C(25)	1.480(3)	N(2P)Sm(1)S(21)	82.69(5)
N(21)–C(22)	1.481(3)	S(11)Sm(1)S(21)	85.93(2)
N(31)–C(31)	1.324(3)	S(22)Sm(1)S(21)	62.11(2)
N(31)–C(35)	1.476(3)	S(31)Sm(1)S(21)	85.35(2)
N(31)–C(32)	1.477(3)	S(12)Sm(1)S(21)	119.54(2)
C(1S)–Cl(1S)	1.745(7)	S(32)Sm(1)S(21)	132.68(2)
C(1S)–Cl(2S)	1.736(7)	Cl(2S)C(1S)Cl(1S)	112.6(4)

* The C–C bond lengths in 2,2'-Bipy are 1.362(4)–1.399(3) Å, and the C–C bond lengths in the C_4H_8N cycles are 1.387(5)–1.520(5) Å.

deposit@ccdc.cam.ac.uk or http://www.ccdc.cam.ac.uk/data_request/cif) and are available from the authors.

X-ray phase analyses of polycrystals of compounds **I**–**V** were carried out on a Shimadzu XRD-7000 diffractometer (CuK_α radiation, Ni filter, 2θ range 5°–60°, increment 0.02°, accumulation 5 s in point). Samples for the study were prepared as follows. Polycrystals were triturated in an agate mortar in the presence of heptane, and the obtained suspension was deposited on the polished side of a standard quartz cell. After heptane was evaporated, the sample represented a thin smooth layer (thickness ~100 μm). An additional series of recordings was carried out for which samples of the compounds were triturated without heptane and deposited on a quartz cell covered with a thin layer of Nujol. In this case, the accumulation was 1 s in point.

The magnetic susceptibility (χ) of samples of compounds **I**–**V** was measured on an MPMSXL SQUID magnetometer (Quantum Design) in the temperature range from 2 to 300 K at a magnetic field strength of 5 kOe. The paramagnetic components of the magnetic susceptibility were determined taking into account the diamagnetic contribution estimated from Pascal's constants. The effective magnetic moment (μ_{eff}) was calculated by the formula $\mu_{\text{eff}} = [3k\chi T/(N_A\mu_B^2)]^{1/2}$, where N_A, μ_B, and k are Avogadro's number, Bohr's magneton, and Boltzmann's constant, respectively.

The photoluminescence and luminescence excitation spectra of the solid samples of compounds **I**–**V** were recorded on a Cary Eclipse Varian scanning spectrophotometer at 300 K, $V = 800$ V, and a slit width of 5 nm. The PL spectra for compounds **I** and **III** were recorded at $\lambda_{\text{exc}} = 340$ and 314 nm, respectively.

RESULTS AND DISCUSSION

Compounds **I**–**V** are formed in the reaction of Ln^{3+} ions with $C_4H_8NCS_2^-$ ions and 2,2'-Bipy at a mole ratio of 1 : 4 : 1 in an CH_2Cl_2–*iso*-PrOH mixture. The syntheses of compounds **I**–**V** are based on the modified procedure for the synthesis of compound **I** [20]: the stirring time was increased and the solvent volume was decreased, which allowed us to significantly enhance the yield of the substances. According to the chemical analysis data, compounds **I**–**V** have the composition $Ln(2,2'\text{-Bipy})(C_4H_8NCS_2)_3 \cdot 0.5CH_2Cl_2$. The thermal properties of compound **I** were studied as an example for the estimation of the stability of the obtained substances containing CH_2Cl_2. According to thermogravimetry (TG) data, on heating compound **I** a noticeable mass loss started only about 110°C. The TG curve contains three steps. For the first of them (110–200°C), the mass loss is close to 5% corresponding to the loss of CH_2Cl_2 molecules (the calculated content of CH_2Cl_2 in compound **I** is 5.4%). The mass loss completes about 550°C. The sample of compound **I** was kept at 80–90°C for 48 h. The elemental analysis data for the sample showed that at this temperature no complete removal of CH_2Cl_2 occurred even for such a prolong storage. The data of thermal analysis and thermal storage indicate a sufficiently strong retention of CH_2Cl_2 molecules in the crystal structure of compound **I**.

According to the X-ray diffraction data, the crystal structure of compound **I** consists of molecules of mononuclear complex $[Sm(2,2'\text{-Bipy})(C_4H_8NCS_2)_3]$

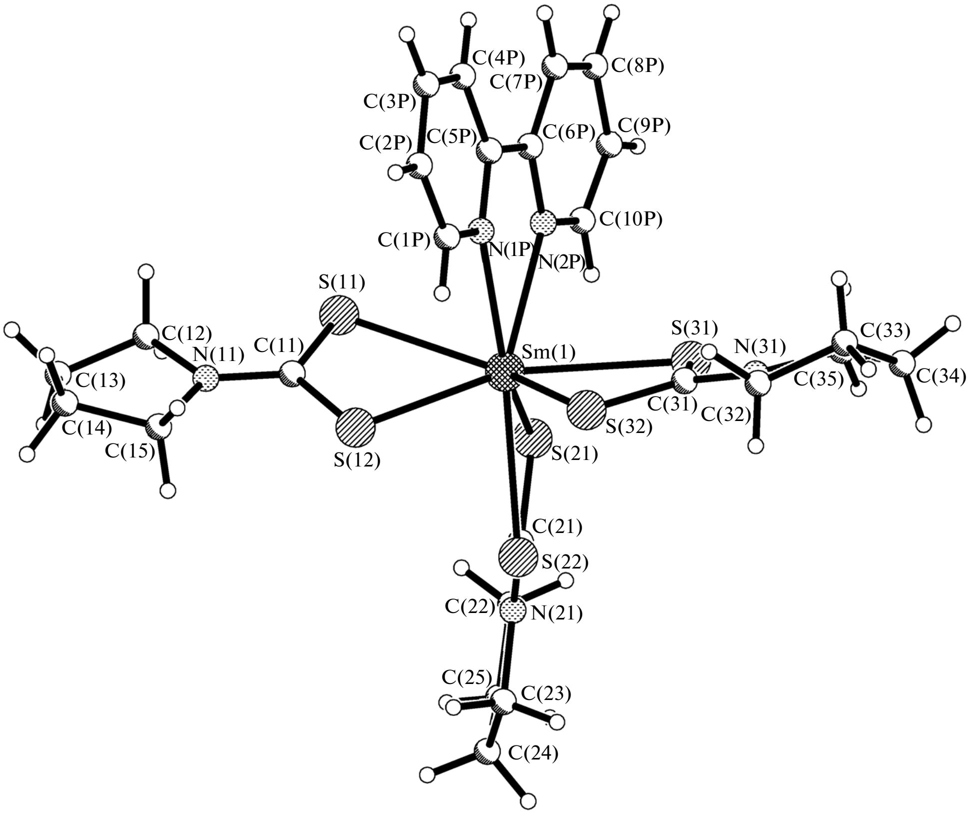

Fig. 1. Molecular structure of [Sm(2,2'-Bipy)($C_4H_8NCS_2$)$_3$] with designations of non-hydrogen atoms.

and disordered solvate CH_2Cl_2 molecules, and one CH_2Cl_2 molecule falls onto two molecules of the complex. The molecular structure of complex **I** is shown in Fig. 1. The coordination sphere of the Sm atom includes two N atoms of the bidentate-chelating ligand 2,2'-Bipy (Sm–N 2.591(2) and 2.608(2) Å) and six S atoms of three bidentate-chelating ligands $C_4H_8NCS_2^-$ (Sm–S 2.8505(6)–2.9042(7) Å). The coordination polyhedron N_2S_6 of the Sm atom is a distorted tetragonal antiprism. The coordination of the ligands affords three four-membered chelates SmS_2C and one five-membered metallocycle SmN_2C_2. The dihedral angles between the SSmS and SCS planes of metallocycles SmS_2C (3.3(1)°, 10.0(1)°, 12.2(1)°) indicate a noticeable deformation of two of them. Chelate SmN_2C_2 is nearly planar with an average deviation of ±0.043(1) Å. Three five-membered pyrrolidine cycles C_4N of the $C_4H_8NCS_2^-$ ligands exist in different conformations. One of the cycles is nearly planar (±0.032(2) Å). Two other cycles have an envelope conformation with the deviations of the C(13) and C(33) atoms from the plane of other four atoms by 0.397(7) and 0.571(6) Å, respectively. The angle of turn of the planar pyridine cycles 2,2'-Bipy around the C(5P)–C(6P) bond relatively to each other (10.07(6)°) does not allow one to consider these cycles as one planar system. The C$\overset{\cdots}{-}$N bond lengths (1.32–1.33 Å) in the $C_4H_8NCS_2^-$ ligands are intermediate between the lengths of standard ordinary and double carbon–nitrogen bonds. The situation is similar for the C$\overset{\cdots}{-}$S bond lengths (1.71–1.73 Å).

The molecular packing of complex [Sm(2,2'-Bipy)($C_4H_8NCS_2$)$_3$] and disordered CH_2Cl_2 molecules in the projection onto the (100) plane is shown in Fig. 2. The values of all intermolecular contacts are at a level of van der Waals interactions, and the shortest S···C contacts of the 2,2'-Bipy ligands are 3.613(4) and 3.625(3) Å. The disordered CH_2Cl_2 molecules with site occupancies of 0.5 are arranged near the symmetry centers between the molecules of the complexes. Since no interactions are observed between the complex and CH_2Cl_2 molecules (the minimum S···C contact is 3.606(7) Å), compound **I** can be assigned to solvates. It is most likely that compounds **II–V** are also solvates.

A comparison of the crystallographic characteristics of the molecular structures of complex [Sm(2,2'-Bipy)($C_4H_8NCS_2$)$_3$] in the composition of solvate **I** and [Sm(2,2'-Bipy)(Et_2NCS_2)$_3$] (**VI**) earlier studied by X-ray diffraction analysis [22] shows that both complexes have the same coordination node SmS_6N_2 with insignificantly differed Sm–S and Sm–N distances. The SmN_2C_2 chelates are nearly planar in both complexes. However, the dihedral angles between the

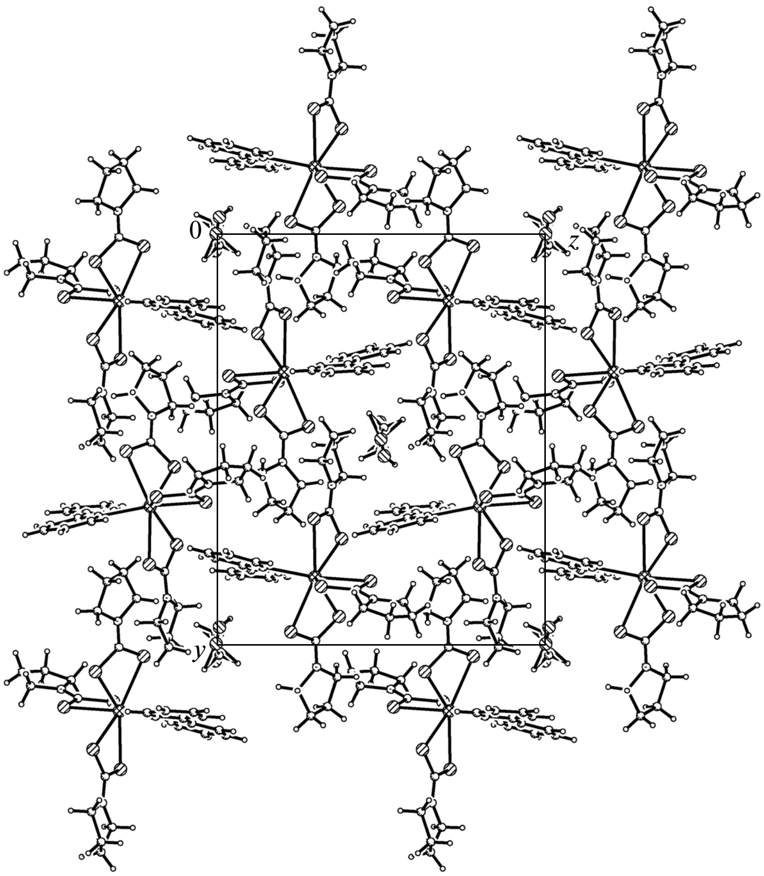

Fig. 2. Molecular packing of [Sm(2,2'-Bipy)($C_4H_8NCS_2$)$_3$] and CH_2Cl_2 in structure **I** in the projection onto the (100) plane.

SSmS and SCS planes in three SmS_2C chelates and the angles of turn of the heterocycles of 2,2'-Bipy molecules differ. In compound **I** the maximum dihedral angle is 12.2° whereas in compound **VI** this angle is much larger (26.8°). The angle of turn of 2,2'-Bipy in complex **I** is equal to 10.1°, whereas in complex **VI** it is somewhat larger (14.4°). Therefore, the replacement of the acyclic fragment Et_2N by heterocyclic C_4H_8N in dithiocarbamate ligands and the presence of CH_2Cl_2 molecules in compound **I** exert no substantial effect on the type of the coordination polyhedron of the Sm atom and on the geometric parameters of molecules of the complex. The difference results only in some change in the unit cell parameters and a slight change in the Sm···Sm distances. For example, the Sm···Sm distance in complex **VI** is 10.518(4) Å, while in solvate **I** it is 11.308(2) Å.

Indexing of the diffraction patterns of compounds **I–V** was performed by analogy to that of the theoretical diffraction pattern of compound **I** obtained from the X-ray diffraction data. The experimental and theoretical diffraction patterns for compound **I** coincided (Fig. 3). The diffraction patterns of the samples prepared by trituration with heptane and without heptane do not differ. Evidently, the composition remained unchanged upon the preparation of the samples of compounds **I–V** for X-ray phase analysis (trituration in heptane). According to the X-ray phase analysis data, the diffraction patterns of compounds **II–V** are similar to that of compound **I** (Fig. 3). The diffraction patterns of compounds **II–IV** contain an unidentified peak of low intensity (θ 7.56°, 9.72°, and 9.73° for **II**, **III**, and **IV**, respectively). The unit cell parameters were refined for all compounds using the PowderCell 2.4 program [23]. The profile of peaks, background, and unit cell parameters were varied, and the peak profiles were described by the pseudo-Voigt function. For the refinement of the unit cell parameters, the space group of compound **I** was transformed into standard $P2_1/c$. The obtained crystallographic parameters for compounds **I–V** (Table 3) indicate that these complexes are isostructural. The difference in unit cell parameters for compound **I** between the powder and single crystal experiments is due to the difference in temperatures: the single crystal experiment was carried out at 150 K and the powder experiment was carried out at 297 K. The decrease in the cell volume from **I** to **V** corresponds to the lanthanide contraction.

The bands corresponding to vibrations of the CS_2 and CN groups in ligand $C_4H_8NCS_2^-$ were identified in

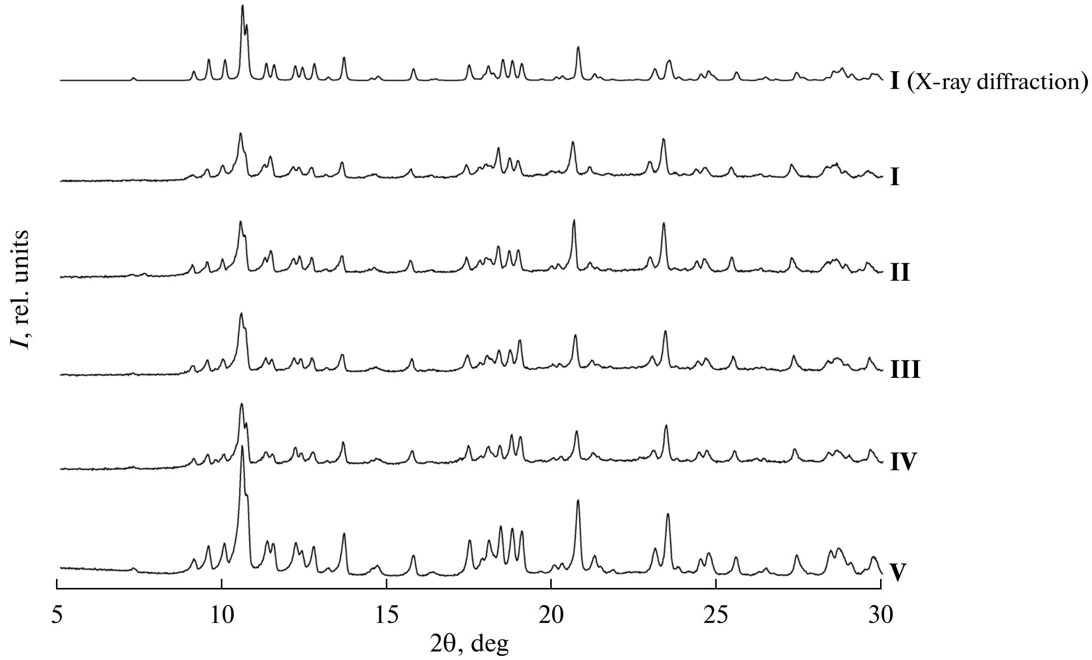

Fig. 3. Experimental diffraction patterns of compounds **I–V** and the theoretical diffraction pattern of compound **I** (X-ray diffraction).

the IR spectrum of compound **I** (Table 4) [24]. Similar bands in the spectra of compounds **II–V** confirm the bidentate-chelating coordination mode of ligand $C_4H_8NCS_2^-$ in these compounds. The band $\nu(CS_2)$ in the spectra of compounds **I–V** is shifted toward high frequencies compared to its position in the spectrum of $C_4H_8NCS_2NH_4$, indicating the coordination of the CS_2 fragment in compounds **I–V**.

The dependences $\mu_{eff}(T)$ for compounds **I–V** are presented in Fig. 4. At 300 K the values of μ_{eff} are 1.85, 3.40, 10.7, 9.75, and 7.91 μ_B for compounds **I–V**, respectively. For compounds **I** and **II**, the values of μ_{eff} at 300 K are consistent with the experimental values for the complexes of Sm^{3+}, Eu^{3+} ions [25]. The dependences $\mu_{eff}(T)$ for compounds **I** and **II** differ substantially from those for compounds **III–V**. For compounds **I** and **II**, as the temperature decreases, μ_{eff} decreases gradually to 0.57 and 0.58 μ_B at 5 K due to a decrease in the site occupancies of the excited states closely arranged in energy to the ground state ($^6H_{5/2}$, $g = 2/7$ for Sm^{3+} and $^7F_0$ for Eu^{3+}). An analysis of the $\mu_{eff}(T)$ dependence using the equation for the magnetic susceptibility in the free ion approximation [26] gave the value of the spin–orbital interaction parameter λ for compound **II**. The optimum value of λ (299 ± 3 cm^{-1}) is consistent with a value of 314 (±3) cm^{-1} for complex $Eu(Phen)(C_4H_8NCS_2)_3$ that is similar in structure to complex **II** [19]. In the case of compounds **III–V**, the excited states are much higher in energy and, hence, the magnetic properties are determined by the ground state only. The values of μ_{eff} for compounds **III–V** remain almost unchanged with the temperature decrease to 50 K and agree with the theoretical values for the ground state (9.72 μ_B-$^7F_6$, $g = 3/2$ for Tb^{3+}; 10.66 μ_B-$^6H_{15/2}$, $g = 4/3$ for Dy^{3+}; 7.56 μ_B-$^3H_6$, $g = 7/6$ for Tm^{3+}). The slight decrease in μ_{eff} for compounds **III–V** with the temperature

Table 3. Crystallographic characteristics of compounds **I–V**

Compound	a, Å	b, Å	c, Å	β, deg	V, Å^3
I(X-ray diffraction)*	10.1401(3)	19.5406(7)	17.1343(4)	113.428(1)	3115.18
I	10.214(2)	19.641(3)	17.256(3)	113.62(2)	3171.82
II	10.213(2)	19.637(3)	17.237(3)	113.60(2)	3167.90
III	10.200(2)	19.597(3)	17.196(3)	113.59(2)	3150.02
IV	10.192(2)	19.577(3)	17.169(3)	113.61(2)	3138.80
V	10.176(2)	19.542(3)	17.137(3)	113.60(2)	3122.88

*The parameters are presented for the cell transformed into the $P2_1/c$ group.

Table 4. Main vibrational frequencies (cm^{-1}) in the IR spectra of $C_4H_8NCS_2NH_4$ and compounds **I–V**

Assignment	$C_4H_8NCS_2NH_4$	**I**	**II**	**III**	**IV**	**V**
$\nu(\mathrm{C}\overset{\cdots}{-}\mathrm{N})$	1416, 1377	1427	1430	1429	1420	1425
$\nu(\mathrm{CS_2})$	990	1008	1008	1010	1005	1006

decrease below 50 K is due to the splitting in the zero field typical of lanthanide ions. The nonlinear dependence of the magnetization of the sample on the external magnetic field strength is observed for complex **IV** at 2 K (Fig. 5). The value of spontaneous magnetization ($\boldsymbol{\sigma_0}$) obtained from an analysis of the dependence $\sigma = \sigma_0 + \chi H$ at $H > 20$ kOe, where χ is the magnetic susceptibility of the sample and H is the intensity of the applied magnetic field, is 27100 (±130) G cm^3/mol^{-1}.

Under UV irradiation, only compounds **I** and **III** exhibit PL in the visible spectral range. We failed to detect the PL spectra for other compounds because of the very low intensity (I) of PL. For recording the PL spectra of compounds **I** and **III**, we chose exciting wavelengths of 340 and 314 nm corresponding to maxima in the luminescence spectra of the compounds (Fig. 6). The spectrum of compound **I** contains four bands at 564, 601, 647, and 705 nm corresponding to the transitions $^4G_{5/2} \to {}^6H_{5/2}, \to {}^6H_{7/2}, \to {}^6H_{9/2}, \to {}^6H_{11/2}$, respectively (Fig. 6). The red band at 647 nm has the maximum value of I. The values of λ_{max} of the bands coincide with the data for $Sm(Phen)(C_4H_8NCS_2)_3$ [19]. The PL of compound **III** contains bands at 489, 544, 585, and 621 nm corresponding to the transitions $^5D_4 \to {}^7F_6, \to {}^7F_5, \to {}^7F_4$, and $\to {}^7F_3$, respectively. The green band with λ_{max} = 544 nm is the most intense in the spectrum of compound **III** (Fig. 6). The value of I of the red band (compound **I**) is almost 14 times higher than I of the green band (**III**). The fact that the Sm(III) compound has the highest PL intensity in a series of compounds **I–V** agrees with the data on the PL of complexes $Ln(Phen)(Et_2NCS_2)_3$ (Ln = Pr, Sm, Eu, Tb, and Dy) [14] and $Ln(Phen)(C_4H_8NCS_2)_3$ (Ln = Sm, Eu, Tb, Dy, and Tm) [19]. It was found for these compounds that the Sm(III) complexes have the highest PL intensity. Evidently, the replacement of Phen by 2,2'-Bipy results in the same specific feature of the PL of the Sm(III) compound. The presence of CH_2Cl_2 molecules in compounds **I** and **III** exerts no effect on this tendency. It is most likely that the high PL intensity of the Sm(III) complexes containing the nitrogen heterocycle and dithiocarbamate ions is due to the optimum arrangement of electron levels of the ligands and Sm^{3+} ion relatively to each other, resulting in the efficient PL of the Sm(III) complexes.

ACKNOWLEDGMENTS

The authors are grateful to A.P. Zubareva and O.S. Koshcheeva for the elemental analysis data, to

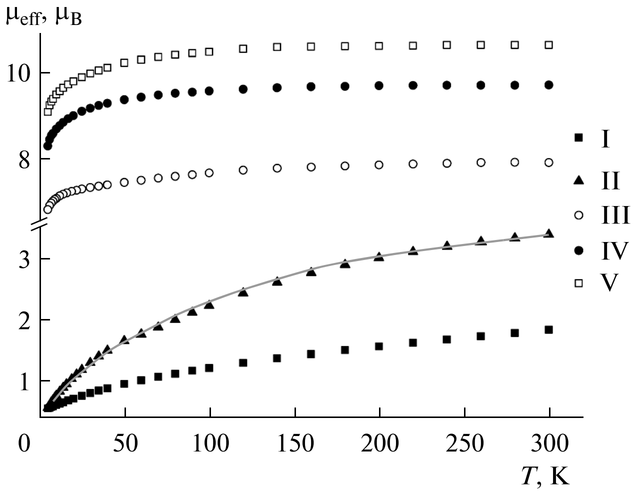

Fig. 4. Dependences $\mu_{eff}(T)$ for compounds **I–V** (points are experimental data, and solid line is the theoretical curve).

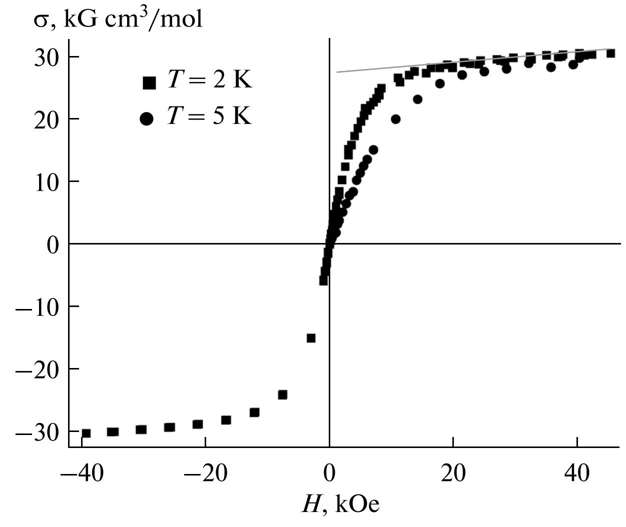

Fig. 5. Magnetization vs. external magnetic field strength for compound **IV** (points are experimental data, and solid line is the theoretical curve).

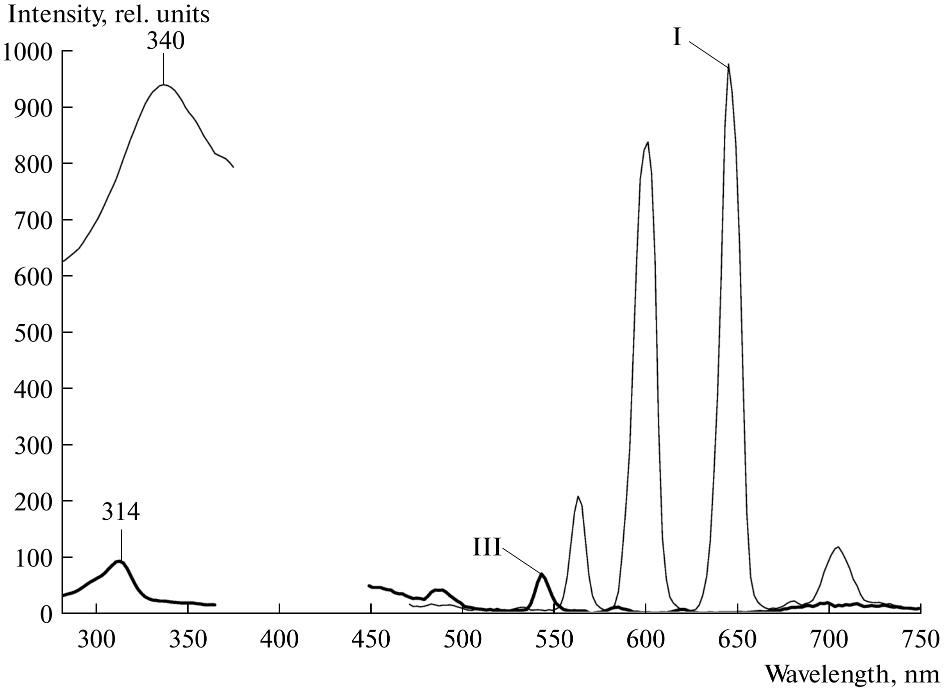

Fig. 6. Photoluminescence and luminescence excitation spectra for compounds **I** (λ_{exc} = 340 nm) and **III** (λ_{exc} = 314 nm).

P.E. Plyusnin for the thermogravimetry data, and to N.I. Alferova for recording the IR spectra.

REFERENCES

1. De Sa, G.F., Malta, O.L., de Mello Donega, C., et al., *Coord. Chem. Rev.*, 2000, vol. 196, no. 1, p. 165.
2. Bunzli, J.-C.G., *Acc. Chem. Res.*, 2006, vol. 39, no. 1, p. 53.
3. Metelitsa, A.V., Burlov, A.S., Bezuglyi, S.O., et al., *Rus. J. Coord. Chem.*, 2006, vol. 32, no. 12, p. 858.
4. Armelao, L., Quici, S., Barigelletti, E., et al., *Coord. Chem. Rev.*, 2010, vol. 254, nos 5–6, p. 487.
5. Bochkarev, M.N., Vitukhnovskii, A.G., and Katkova, M.A., *Organicheskie svetoizluchayushchie diody (OLED)* (Organic Light-Emitting Diodes), Novgorod: Dekom, 2011.
6. Kumar, G.A., Riman, R.E., Diaz Torres, L.A., et al., *Chem. Mater.*, 2005, vol. 17, no. 20, p. 5130.
7. Banerjee, S., Huebner, L., Romanelli, M.D., et al., *J. Am. Chem. Soc.*, 2005, vol. 127, no. 45, p. 15900.
8. Katkova, M.A., Borisov, A.V., Fukin, G.K., et al., *Inorg. Chim. Acta*, 2006, vol. 359, no. 13, p. 4289.
9. Katkova, M.A., Ilishev, V.A., Konev, A.N., et al., *Organic Electronics*, 2009, vol. 10, no. 4, p. 623.
10. Kobayashi, T., Naruke, H., and Yamase, T., *Chem. Lett.*, 1997, vol. 26, no. 9, p. 907.
11. Su, C.G., Tan, M.Y., Tang, N., et al., *J. Coord. Chem.*, 1996, vol. 38, no. 3, p. 207.
12. Varand, V.L., Glinskaya, L.A., Klevtsova, R.F., and Larionov, S.V., *Zh. Strukt. Khim.*, 1998, vol. 39, no. 2, p. 300.
13. Faustino, W.M., Malta, O.L., Teotonio, E.E.S., et al., *J. Phys. Chem. A*, 2006, vol. 110, no. 7, p. 2510.
14. Regulacio, M.D., Publico, M.H., Vasquez, J.A., et al., *Inorg. Chem.*, 2008, vol. 47, no. 5, p. 1512.
15. Meng, X.-X., Gao, S.-L., Chen, S.-P., et al., *Acta Chim. Sinica*, 2004, vol. 62, no. 22, p. 2233.
16. Chen, S.P., Meng, X.X., Shuai, Q., et al., *J. Therm. Anal. Cal.*, 2006, vol. 86, no. 3, p. 767.
17. Chen, S.P., Gao, S.L., Yang, X.W., et al., *Rus. J. Coord. Chem.*, 2007, vol. 33, no. 3.
18. Selinsky, R.S., Han, J.H., Morales Perez, E.A. et al., *J. Am. Chem. Soc.*, 2010, vol. 132, no. 45, p. 15997.
19. Bryleva, Yu.A., Glinskaya, L.A., Korol'kov, I.V., et al., *J. Struct. Chem.*, 2014, vol. 55, no. 2, p. 319.
20. Bryleva, Yu.A., Kokina, T.E., Uskov, E.M., et. al., *Rus. J. Coord. Chem.*, 2013, vol. 39, no. 1, p. 41.
21. Sheldrick G.M., *SHELXS-97 and SHELXL-97. Programs for the Refinement of Crystal Struñtures*, Gottingen (Germany): Univ. of Gottingen, 1997.
22. Varand, V.L., Glinskaya, L.A., Klevtsova, R.F., and Larionov, S.V., *Zh. Strukt. Khim.*, 2000, vol. 41, no. 3, p. 663.
23. Kraus, W., Nolze, G., *J. Appl. Cryst.*, 1996, vol. 29, no. 3, p. 301.
24. Byr'ko, V.M., *Ditiokarbamaty* (Dithiocarbamates), Ìoscow: Nauka, 1984, p. 61.
25. Cotton, S. *Lanthanide and Actinide Chemistry*, Chichester: Wiley, 2006, p. 65.
26. Andruh, M., Bakalbassis, E., Kahn, O., et al., *Inorg. Chem.*, 1993, vol. 32, no. 9, p. 1616.

Translated by E. Yablonskaya